# Study of a Resonant DC/DC Converter in Alternate Discontinuous Mode

Caitríona E. Sheridan, Michaël M.C. Merlin and Timothy C. Green
Control and Power Research Group
Imperial College London, London, UK
c.sheridan11@ic.ac.uk

***Abstract*— This paper looks at DC to DC conversion for high power applications. After having briefly reviewed the domain, a resonant bidirectional DC/DC converter already suggested in the literature is closely studied using a novel mode of operation, dubbed Alternate Discontinuous Mode. This operating mode alternates the two halves of the converter in such a way that the two DC grids are never connected. This alternative operating principle ensures the converters fault blocking capabilities and, by operating in discontinuous conduction mode, the switching losses are minimized. This operation principle is presented and subsequently confirmed through simulation of different DC grid scenarios that would necessitate the use of a DC/DC converter, using either highly rated or fast switching thyristors.**

***Index Terms*—DC/DC Conversion, DC-DC Power Converters, HVDC, Multiterminal Grid**

## I. INTRODUCTION

It has been proposed that a HVDC SuperGrid could connect the offshore wind generation from the North Sea to the potential solar generation in southern Europe and northern Africa, geothermal generation in Iceland, and hydro generation in Norway [1]. It has been long established that this SuperGrid will be implemented using HVDC transmission, as it is more efficient and cost-effective than HVAC over significant distances. Furthermore Voltage Source Converter (VSC) technology is better suited for multiterminal HVDC (MTDC) networks than classic line commutated converters, as reversing the power flow is done through changing current polarity, whereas the latter does this by reversing voltage polarity. The main restrictions with realizing a MTDC grid have been the lack of a commercially available DC circuit breaker and the current power ratings of VSC technology [2], [3]. However a hybrid DC circuit breaker has been proposed and a prototype has been successfully tested at 80 kV, [4]. There have also been VSC converters presented that have the ability to block DC faults [5].

Currently there is no established grid code for a MTDC grid, and as cable ratings increase by tens of kilovolts at each iteration of the technology, newer projects will be constructed using the latest technology and adjacent systems may be operated at different voltage levels. A DC/DC converter would allow DC systems of different voltage levels to be interconnected. They could also allow systems from differing manufacturers to be connected and allow interconnection between classic HVDC systems, and VSC systems. They would also enable the interconnection of medium or low voltage DC distribution or collection systems to be interfaced with a HVDC grid. Thus the importance of DC/DC conversion to realize a MTDC grid is paramount. It has been established that one DC/DC converter topology will not suit every application, and that different converters must be considered for different applications in a MTDC grid [6].

This paper will give a brief overview of DC/DC conversion methods. A bidirectional resonant, thyristor based, DC/DC converter is studied in detail and is implemented using an alternative operating principle to that discussed in [7]. This operating principle is described theoretically, and is then verified through simulation of three scenarios, using two different thyristor types. A loss calculation study is then carried to determine the conduction losses of the semiconductor devices of the converter.

## II. DC/DC CONVERSION

There are two ways of converting DC as illustrated in Fig. 1: (1) by using two AC/DC converters connected through the AC stage, (2) through a dedicated DC/DC converter using power electronics.

### *A. DC/AC/DC Conversion*

AC/DC converters have been studied and commissioned for several decades [8], thus DC/AC/DC systems benefit from this accumulated knowledge. Some topologies have already been suggested in [6], [9]. Depending on the topology, an AC transformer can be fitted inside the AC connection to provide both galvanic isolation between the two DC buses and boost the voltage conversion ratio. Furthermore, the AC interconnection provides a convenient means to isolate the

The authors gratefully acknowledge the financial support of the Research Councils UK, through the HubNet project (grant number: EP/I013636/1) and through the Control for Energy and Sustainability project (grant number: EP/G066477/1)

circuit when necessary. This implies that DC/AC/DC systems are inherently strong against DC-side faults because they can always shut down their AC subsystem.

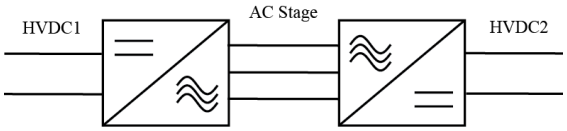


a) DC/AC/DC Converter

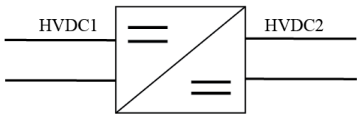


b) Dedicated DC/DC Converter

Figure 1: DC/DC conversion methods

### B. *Dedicated DC/DC Converters*

Another approach to DC/DC conversion consists in using dedicated power electronic converter topologies. Switched Mode Power Supplies (SMPS) have been widely used and optimized for low to medium power applications but exhibits unsatisfying power efficiency, limited voltage conversion ratio and challenging scalability [10]. A recent stream of DC/DC converter topologies for high power applications based on resonant components has had focused research efforts [11], [12]. This class of converters uses the natural oscillation occurring between a capacitor and an inductor in order to transfer energy between the different parts of the circuit. Furthermore by using the zero-crossing points of the current waveforms as switching off points, thyristor switches can be used instead of IGBTs, thus lowering the overall power losses.

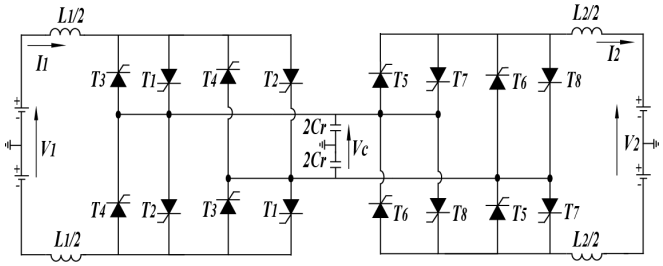


Figure 2: Bidirectional resonant DC/DC converter

A family of resonant converters have been presented in [7], [12]. One circuit in this family is a bidirectional DC/DC converter, shown in Fig. 2, which reverses power flow by changing the current polarity making it suitable for use in VSC based HVDC systems. Given the symmetry of the circuit, this topology might be compatible as well with the voltage polarity reversibility of CSCs. In [7] and [12], the working mechanism has been designed such that both sides of the converter run simultaneously. This method has the advantage of reducing the peak voltage occurring across the middle capacitor, which has a direct influence on the number of devices in series, but also means that fault isolation might be compromised under certain operating conditions [13].

## III. Alternate Discontinuous Mode Operation

### A. *Description*

An alternative operating principle has been derived for this converter topology, termed as alternate discontinuous mode (ADM). This principle involves charging the capacitor through the input inductor, $L_1$, and subsequently discharging through the output inductor, $L_2$, meaning that while one bridge of the converter is on, the other one is off. The converter is also operated in discontinuous conduction mode (DCM) to minimise switching losses. Fig. 3 shows example current waveforms of the converter in ADM.

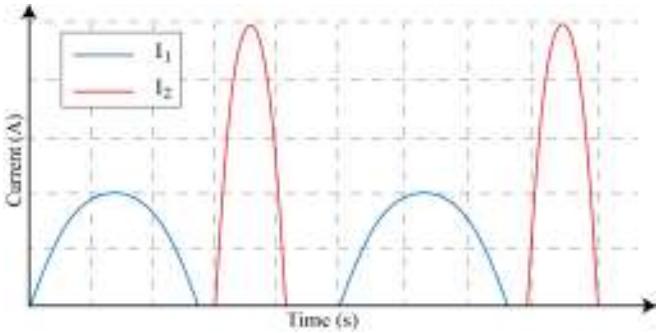


Figure 3: ADM current waveforms

In this mode, the DC/DC converter is operated as two separate LC circuits which alternate in order to transfer a fixed charge of energy from one side to the other one. The advantages are twofold. First, the description of the system is much simplified, leading to a simple control mechanism. Second, at no given point of time, are the two halves of the topology are connected together, avoiding the propagation of a fault current in case of the collapse of one of the DC buses.

### B. *Basic LC Circuit*

By studying the operation of a basic LC circuit, as illustrated in Fig.4, the operation of the ADM can be developed. At $t=0$, the inductor current is equal to zero and the capacitor voltage is equal to $V_0$. The natural pulsation of this circuit is defined by $1/\sqrt{LC}$.

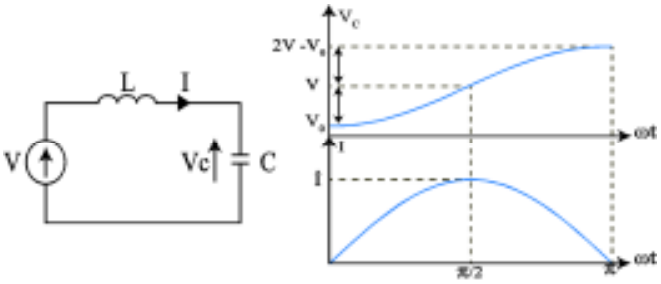


Figure 4: Basic LC circuit and waveforms

At the end of the first half period, the current comes back to zero (1) and the capacitor voltage $V_C$ has increased by two times the voltage difference with the voltage source $V$ defined in (2).

$$\hat{I} = C\,\omega(V - V_0) = \sqrt{\frac{C}{L}}(V - V_0) \tag{1}$$

$$\hat{V}_C = 2V - V_0 \tag{2}$$

*C. Full Model*

The complete DC/DC converter operated in ADM is only an extension from the basic LC circuit with the middle capacitor being connected sequentially to the following voltage over one cycle:

- $V_1$ with $L_1$ through the action of $T_1$ or $T_3$
- $V_2$ with $L_2$ through the action of $T_5$ or $T_7$
- - $V_1$ with $L_1$ through the action of $T_2$ or $T_4$
- - $V_2$ with $L_2$ through the action of $T_6$ or $T_8$

From the list above, the middle capacitor voltage will fluctuate between four voltage points. Control action or parallel resistive losses will centre the final waveform around zero volts, yielding the starting condition for $V_0$ as in (3).

$$V_0 = V_1 - V_2 \tag{3}$$

As a result, the peak voltage of the middle capacitor is equal to the sum of the two DC bus voltages, as shown in (4). This value is essential as it dictates the number $N$ of semiconductor devices connected in series in order to support this voltage.

$$\hat{V}_C = 2V_1 - V_0 = V_1 + V_2 \tag{4}$$

Knowing the voltage waveform of the capacitor voltage, the peak currents can be obtained, as shown in (5) and (6).

$$\hat{I}_1 = C_r\,\omega_1(V_1 - V_0) = \sqrt{\frac{C_r}{L_1}}V_2 \tag{5}$$

$$\hat{I}_2 = C_r\,\omega_2(V_0 - V_2) = \sqrt{\frac{C_r}{L_2}}V_1 \tag{6}$$

Assuming that the transfer of energy between the different parts of the converter is lossless, the power transfer is defined by the amount of energy per half-cycle multiplied by the frequency, as in (7), based on the initial capacitor voltage from (3).

$$P = 2Ef = 4\,C\,V_1\,(V_1 - V_0)\,f = 4\,C\,V_1\,V_2\,f \tag{7}$$

Equation (7) shows that the power transfer depends on the frequency at which the converter is operated. This frequency is set by the varying the delay between the set of pulses sent to either side of the converter to initiate a transfer of charge. The maximum frequency at which this topology can run in ADM is defined by the inverse of the sum of the time lengths of both resonant periods, as shown in (10). The topology can be operated past this value in order to boost the power transfer but at the expense of even more power losses as the converter will switch into CCM, thus the switching losses will start to become significant.

$$T_1 = \frac{\pi}{\omega_1} = \pi\sqrt{L_1 C_r} \tag{8}$$

$$T_2 = \frac{\pi}{\omega_2} = \pi\sqrt{L_2 C_r} \tag{9}$$

$$f_{max} = \frac{1}{T_1 + T_2} = \frac{f_1 f_2}{f_1 + f_2} = \frac{1}{2\pi\sqrt{C_r}(\sqrt{L_1} + \sqrt{L_2})} \tag{10}$$

Since the current naturally comes back to zero at the end of each resonant half-cycle, the switches are operated in soft-switching mode. As a result, the switching losses can be ignored. The dominant power losses are thus the conduction losses. Using the current waveforms derived from the results above, together with the on-state voltage $V_{T0}$ and resistance $R$ of the switches and their number $N$.

$$P_C = 2fC_rN\left(\pi R\sqrt{\frac{C_r}{L_2}}V_1^2 + \pi R\sqrt{\frac{C_r}{L_1}}V_2^2 + 4V_{T0}V_1 + 4V_{T0}V_2\right) \tag{11}$$

The values for the passive components are obtained in two steps. First, the middle capacitor is obtained by using (7) with the DC network voltages, the rated power of the station and the maximum frequency. The two last parameters are fixed by the ratings of the chosen semiconductor devices. Second, the inductors have to be chosen such that the maximum frequency (10) is attained. Since this makes only one equation for two variables, the remaining degree of freedom is used to minimize the conduction losses given in (11). Equations (12) and (13) give the resulting values for $L_1$ and $L_2$.

$$L_1 = \left(\frac{1}{2\pi f_M\sqrt{C_r}}\frac{V_2}{V_1 + V_2}\right)^2 \tag{12}$$

$$L_2 = \left(\frac{1}{2\pi f_M\sqrt{C_r}}\frac{V_1}{V_1 + V_2}\right)^2 \tag{13}$$

Remarkably, when using these inductor values, the two peak currents are equal:

$$\hat{I}_1 = \hat{I}_2 = 2\pi f_M C(V_1 + V_2) \tag{14}$$

As the inductor values mainly depend on the ratio between V1 and V2, a large voltage conversion ratio will result in one inductor being really small. The resulting resonance frequency might be too high for the semiconductor device, thus some compromises should be made between switching frequency and power losses.

## IV. Simulations and Loss Calculations

Three test scenarios were chosen and details are given in Table 1. For each scenario a fast thyristor and a phase control thyristor was used to enable a comparison between the switching frequency and the power transfer of the converter. The voltage ratios chosen correspond to cases seen in [9], [14]. The converter model for each scenario was arranged as in Fig. 2 and was implemented using MATLAB Simulink.

These specific thyristors were chosen as the fast thyristor can be operated in the kilohertz range, reducing the size of the resonant components, and the phase control thyristor with its significantly higher voltage and current ratings can enable higher power transfer with fewer devices. For the loss calculation only the conduction loss of the thyristors was considered, as the device is soft-switched the switching losses of the converter were assumed to be negligible.

Table 1: Test scenarios and converter data

| **Thyristor** | | ***5STF 11F3010*** | ***5STP 42U6500*** |
|---|---|---|---|
| ***Optimum frequency*** | | *5 kHz* | *500 Hz* |
| ***Maximum voltage*** | | *6.5 kV* | *3 kV* |
| ***Rated voltage*** | | *3.5 kV* | *1.5 kV* |
| ***Case A*** ***±2.5 kV*** ***±150 kV*** | Power | *5 MW* | *20 MW* |
| | $L_1$ | *2.7 mH* | *6.9 mH* |
| | $L_2$ | *0.65 mH* | *1.6 mH* |
| | C | *0.14 µF* | *6.7 µF* |
| | N | *204* | *88* |
| ***Case B*** ***±25 kV*** ***±150 kV*** | Power | *50 MW* | *240 MW* |
| | $L_1$ | *1.71 mH* | *9.3 mH* |
| | $L_2$ | *0.19 mH* | *0.26 mH* |
| | C | *0.33 µF* | *8.0 µF* |
| | N | *134* | *100* |
| ***Case A*** ***±150 kV*** ***±250 kV*** | Power | *300 MW* | *1.2 GW* |
| | $L_1$ | *4.0 mH* | *9.9 mH* |
| | $L_2$ | *1.4 mH* | *3.6 mH* |
| | C | *0.1 µF* | *4.0 µF* |
| | N | *534* | *229* |

### A. Low-Voltage DC Distribution to HVDC Grid

This scenario is, for example, when a single DC/DC converter is used to connect multiple low-voltage DC devices to a HVDC network. For example, the connection of several photovoltaic arrays, which produce a low voltage DC output, to a HVDC grid would necessitate the use of high step DC/DC converter. In this case, the values of the inductors have been modified compared to the optimal results from (12) and (13) because the high stepping ratio resulted in very small values for $L_2$, leading to a second resonant period too short compared to the extinction time of the thyristors.

### B. Medium-Voltage Distribution to HVDC Grid

This scenario is for when a DC collection system, at a medium voltage, is connected to a HVDC grid. An example of this would be if an offshore wind farm made use of a medium-voltage DC collection network, necessitating a step-up DC/DC conversion to the HVDC network.

### C. Interfacing of Two HVDC Systems

As cable technology improves and voltages increase by tens of kilovolts, new HVDC systems will built using the latest technology, implying adjacent projects may not be operated at similar voltage levels. These projects can be interconnected through DC/DC conversion.

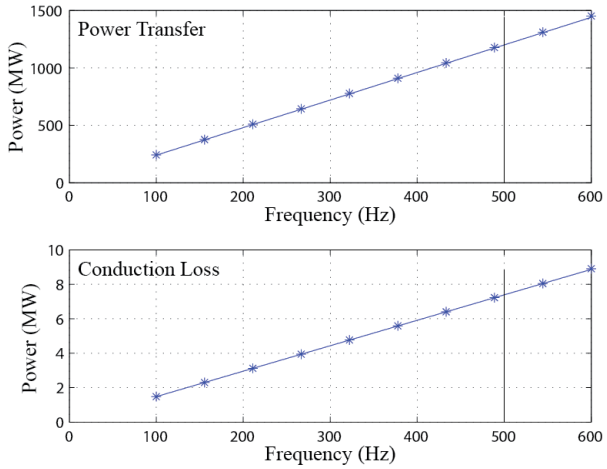


Figure 5: Relationship between frequency and power

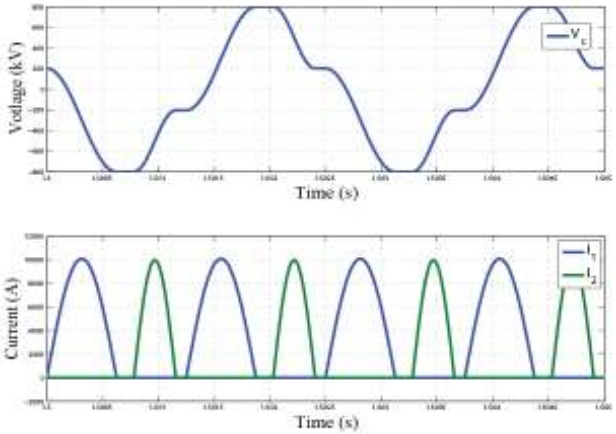


Figure 6: Waveforms of low voltage ratio converter operating at 400 Hz

### D. Results and Discussion

Fig. 5 shows the data from the simulations at different frequency and the prediction from (7) and (11). The close match between the data points and the model proves the linear relationship between switching frequency and the power transfer, and the conduction loss. The converter has also been operated past the set maximum frequency, i.e. 500 Hz, and shows that extra power transfer can be obtained if necessary. Fig. 6 shows the voltage across the capacitor and the currents through the inductor when operating at 400 Hz with a power transfer of approximately 1 GW.

Table 2 shows the relationship between the switching frequency and power transfer and conduction power loss for the three scenarios for both thyristors. The conduction ratio is the ratio of the conduction loss to the power transfer for the converter and, according to the model (7) and (11), is equal independent from the frequency, as long as the converter is operated in ADM.

Table 2: Simulation results

| **Thyristor** | | ***5STF 11F3010*** | ***5STP 42U6500*** |
|---|---|---|---|
| ***Case A*** | P | *1 kW/Hz* | *40 kW/Hz* |
| | Pc | *218 W/Hz* | *3.45 kW/Hz* |
| | *Pc/P* | *21.8%* | *8.6%* |
| ***Case B*** | P | *10 kW/Hz* | *480 kW/Hz* |
| | Pc | *184.22 W/Hz* | *5.29 kW/Hz* |
| | *Pc/P* | *1.8%* | *1.1%* |
| ***Case C*** | P | *600 kW/Hz* | *2.4M W/Hz* |
| | Pc | *911 W/Hz* | *14.77 kW/Hz* |
| | *Pc/P* | *1.5%* | *0.6%* |

From these results, it can be seen that the linear relationship is confirmed between the switching frequency and the power transfer and conduction loss of the device. It was also observed from simulations that conduction losses decrease as the voltage conversion ratio is reduced. This makes the converter suitable for use in interfacing two HVDC systems, when operated in ADM. However, for medium to high voltage conversion ratios the exhibits significant conduction losses deeming it unsuitable for use in interfacing low-voltage DC systems with a HVDC grid. The results also indicate that the phase control thyristor has superior loss figures and fewer devices per arm given the devices higher ratings, at the expense of larger and possibly more costly passive components.

## V. CONCLUSION

Having outlined the importance of DC to DC conversion in future HVDC networks, a resonant converter topology was studied. An alternative operating principle for this topology was presented, involving an alternate operation of the two halves of the topology. A full set of equations describing the working of the converter running in this mode were drawn and estimation of the conduction losses performed. The converter was modeled in different HVDC grid scenarios to show its potential diversity of applications. It was seen that the converter exhibits low losses at low conversion ratios and is suited best to interfacing HVDC systems up to medium conversion ratio. A comparison between two different types of semiconductors, i.e. high ratings or fast switching thyristors, has also been conducting. On one hand, the higher ratings thyristors exhibit the lowest conduction losses over all the scenarios. On the other hand, the fast switching thyristors permit the converter to be operated at a much higher frequency, potentially having benefits in terms of passive components volume and cost.

## REFERENCES


[1] D. Van Hertem, M. Ghandhari, and M. Delimar, "Technical limitations towards a SuperGrid — A European prospective," in *2010 IEEE International Energy Conference*, 2010, pp. 302–309.

[2] D. Van Hertem, M. Ghandhari, J. Curis, O. Despouys, and A. Marzin, "Protection requirements for a multi-terminal meshed DC grid," *Cigre Conference Bologna 2011*, pp. 1–4.

[3] C. M. Franck, "HVDC Circuit Breakers: A Review Identifying Future Research Needs," *IEEE Transactions on Power Delivery*, vol. 26, no. 2, pp. 998–1007, Apr. 2011.

[4] J. Häfner and B. Jacobson, "Proactive Hybrid HVDC Breakers - A key innovation for reliable HVDC grids," *The electric power system of the future - Integrating supergrids and microgrids International symposium - Cigré*, 2011.

[5] M. M. C. Merlin, T. C. Green, P. D. Mitcheson, D. R. Trainer, D. R. Critchley, and R. W. Crookes, "A new hybrid multi-level voltage-source converter with DC fault blocking capability," in *9th IET International Conference on AC and DC Power Transmission (ACDC 2010)*, 2010, pp. 1–5.

[6] C. D. Barker, C. C. Davidson, D. R. Trainer, and R. S. Whitehouse, "Requirements of DC-DC Converters to facilitate large DC Grids," in *Cigre Session 2012*, 2012.

[7] D. Jovcic, "Step-up DC–DC converter for megawatt size applications," *IET Power Electronics*, vol. 2, no. 6, p. 675, 2009.

[8] J. Arrillaga, *High Voltage Direct Current Transmission*, 2nd ed. The Institution of Electrical Engineers, 1998.

[9] T. Lüth, M. M. C. Merlin, T. C. Green, C. D. Barker, F. Hassan, R. W. Critchley, R. W. Crookes, and K. Dyke, "Performance of a DC / AC / DC VSC System to Interconnect HVDC Systems," in *10th IET International Conference on AC and DC Power Transmission (ACDC 2012)*, 2012, no. Figure 2.

[10] N. Mohan, T. M. Undeland, and W. P. Robbins, *Power Electronics: converters, applications, and design*, 3rd ed. 2003.

[11] A. Hagar, "A New Family of Transformerless Modular DC-DC Converters for High Power Applications," University of Toronto, 2011.

[12] D. Jovcic, "Bidirectional, high-power DC transformer," *Power Delivery, IEEE Transactions on*, vol. 24, no. 4, pp. 2276–2283, 2009.

[13] D. Jovcic and B. T. Ooi, "Theoretical aspects of fault isolation on high-power direct current lines using resonant direct current/direct current converters," *IET Generation, Transmission & Distribution*, vol. 5, no. 2, p. 153, 2011.

[14] P. Monjean, J. Delanoe, D. Marin, J. Auguste, C. Saudemont, and B. Robyns, "Control strategies of DC-based offshore wind farm," in *14th European Conference on Power Electronics and Applications (EPE 2011)*, 2011, pp. 1–9.